Electronic structure of titania-based nanotubes investigated by EELS spectroscopy

Alexandre Gloter,[1,2] Christopher Ewels,[1,3] Polona Umek,[4] Denis Arcon,[4,5] and Christian Colliex[1]
[1]*Laboratoire de Physique des Solides, Université Paris Sud, CNRS UMR 8502, F-91405 Orsay, France*
[2]*ICYS, National Institute for Materials Science, Namiki 1-1, Tsukuba 305-0044, Japan*
[3]*Institut des Materiaux, CNRS UMR 6502, 2 rue de la Houssiniere, 44322 Nantes, France*
[4]*Institute "Jozef Stefan," Jamova 39, 1000 Ljubljana, Slovenia*
[5]*Faculty for Mathematics and Physics, University of Ljubljana, Jamova Cesta 2, 1000 Ljubljana, Slovenia*
(Received 11 March 2009; published 10 July 2009)

We present an electron-energy-loss spectroscopy study of the O-K and Ti $L_{2,3}$ edges for anatase-, rutile-, and titania-based nanotubes. The titania-based tubes are composed of tetravalent titanium ions in an octahedral symmetry with the oxygen ligands, however the electronic structure does not correspond to that of either of the titania precursors. Crystal-field splitting is comparable with anatase but the 3*d* occupation number is closer to that of rutile. In addition, Ti $L_{2,3}$ spectroscopic signatures indicate that the octahedron connectivity of the tubes is different to that of the reference titania. We also report the first measurement at the scale of an individual nanometrical object of the charge-transfer satellites for the transition metal 2*p* edges. This may open new opportunities for the estimation of *d*-orbital occupation numbers for transition-metal or rare-earth elements occurring in local grains, phase-segregated regions, nanomaterials, or in the vicinity of interfaces.

DOI: 10.1103/PhysRevB.80.035413 PACS number(s): 79.20.Uv, 61.46.−w, 81.07.De

I. INTRODUCTION

Titanium dioxides such as rutile or anatase are materials of great interest. Rutile is the most widely used white pigment because of its brightness and very high refractive index. Anatase has many others applications including gas detection, catalytic decomposition of toxic materials, and H_2 production via photocatalytic cracking of water.[1] Bulk TiO_2 is a semiconductor with a band gap in the range 3.0–3.2eV depending on the phase. It is photoactive, able to absorb light in the UV which excites an electron-hole pair. The short-lived pair migrates, then catalyzes reactions on the TiO_2 surface via charge transfer.

Recently a large number of papers have reported nanotubes obtained via hydrothermal treatment of titanium oxides. Several structures have been proposed for these tubes, including a scrolling of anatase TiO_2 sheets,[2–4] trititanate $H_2Ti_3O_7$ exfoliated sheets,[5–7] $(Na,H)_2Ti_2O_4(OH)_2$-based layers,[8,9] and lepidocrocite titanatelike sheets.[10] It is currently believed that the structure of these tubes is closely related to the family of layered titanate $H_2Ti_nO_{2n+1}$ materials, where $n=3$, 4, 5, or even ∞ for the end member composed of flat layers of octahedra.[8,10] Although the exact structure is still a matter of debate, all these materials are of the same nature since the published experimental data that are sensitive to structure are identical [in particular, x-ray diffraction and transmission electron microscope (TEM) experiments]. These materials present a large surface area of a few hundreds of $m^2\,g^{-1}$,[11] showing potential for catalytic applications.

In this paper, we investigate by means of electron-energy-loss spectroscopy (EELS) the electronic structure of these titania-based nanotubes, an important aspect when gauging their catalytic properties. Thanks to the high spatial resolution of our dedicated scanning transmission electron microscope (STEM) coupled with an EELS spectrometer,[12] the high-energy excitations can be collected at the scale of an individual nanotube. This limits the occurrence of impurities, unmonitored phases, or imperfect structures that may easily be present from these low-temperature synthesis processes. The electronic structure of these nanotubes is discussed in terms of the titanium formal valence state, the crystal-field splitting, and the hybridization between the transition metal and the ligand anions. Reference anatase and rutile experiments, in combination with calculations based on an Anderson impurity model,[13] are used as a template for the interpretation of the spectroscopic signatures of the nanotube.

II. EXPERIMENTAL METHOD

Nanotubes have been obtained via a hydrothermal treatment process at 135 °C from anatase and sodium hydroxide salt. After repeated washing followed by drying at 100 °C, a white-colored powder is obtained. Our EELS experiments have already shown that very little Na was intercalated after repeated washing cycles.[11] Additional TEM-based experiments such as selected area electron diffraction (SAED), high-resolution electron microscopy (HREM) (see Fig. 1) and energy-dispersive x-ray spectroscopy have also demonstrated that what we called nanotubes for the sake of simplicity are in fact "nanoscrolls," rolled up sheets rather than closed tubes. Based on our TEM and x-ray diffraction studies, these nanotubes are structurally and chemically similar to those obtained by other authors after hydrothermal treatment of a mixture of titanium dioxides and Na(OH) salt, for temperatures constrained under ca. 180 °C. This once again demonstrates the ubiquitous character of these materials.[2–10] More details of the fabrication process, structural aspects, and adsorption properties of the present nanotubes can be found elsewhere.[11] Anatase and rutile nanocrystals have been obtained from reference powders. The structures of these references have been confirmed by means of SAED within the microscope.

 ©2009 The American Physical Society

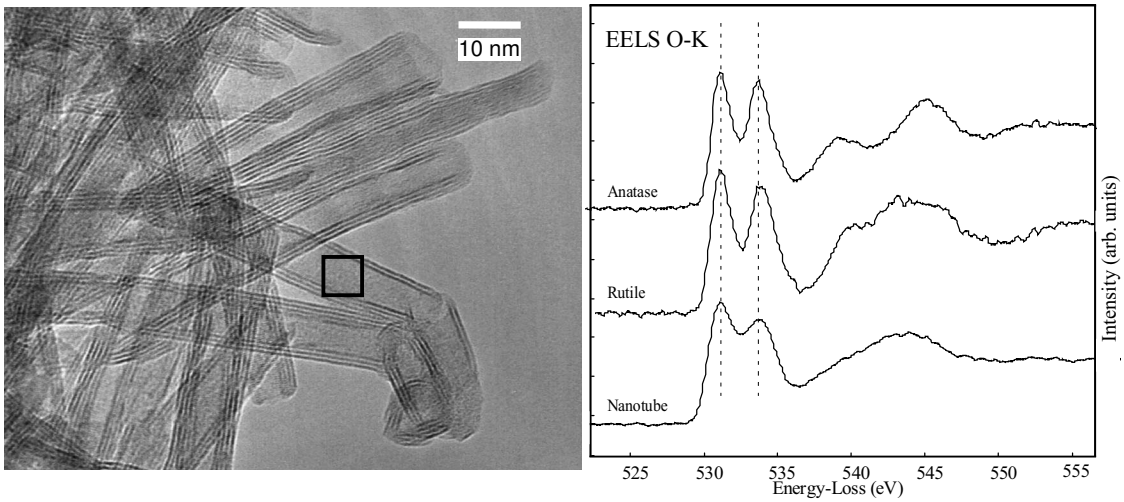

FIG. 1. Left, HREM micrograph of the titanate nanotube. The square indicates the spatial resolution of the EELS spectroscopy. Right, EELS O-K edges for anatase-, rutile-, and the titania-based nanotube. Energy range has been set at 530 eV on the onset of the rutile edge. The dotted lines indicate a 2.5 eV separation.

For the STEM-EELS experiments, titania-based nanotubes, anatase, and rutile nanocrystals have been deposited or codeposited onto TEM grids. Codeposition of two phases is required to measure accurately the chemical shift between Ti $L_{2,3}$ and O-K edges of the different phases. Our STEM-EELS equipment allows the collection of tens of spectra for different phases within a time span of only a few seconds, limiting the energy drift of the spectrometer to less than 0.2 eV. The STEM-EELS data are acquired using a dedicated STEM-VG HB05 (100 keV) and a charge-coupled-device camera-based EELS spectrometer. The natural energy spread of the cold field-emission gun does not exceed 0.5 eV. Time series of hundreds of spectra have been taken. Acquisition time of each individual spectrum was limited to 1 s in order to limit the spectrometer drift and summation over spectra was performed after alignment. Chronospectroscopy shows a stability of the electronic excitations of the nanotubes of several seconds, for electron doses limited to ~200 pA for an analyzed area of ~5 nm^2. The signals are collected at the scale of an individual nanotube (lateral size of ~10 nm). Unfortunately core-EELS excitations at higher spatial resolution (tube walls, defects, or surface states, for instance) are not possible. We believe that at higher-energy doses, the tube structures are altered by the loss of a large quantity of hydroxyl bonding. For Ti $L_{2,3}$ edges in the energy range between 452 and 462 eV, the energy resolution of the spectra has been increased to around 0.3 eV, using a two-dimensional Richardson-Lucy algorithm as described in Ref. 14.

III. RESULTS AND DISCUSSIONS

A. Ti $L_{2,3}$ edges

Figure 2 shows the main peaks of the Ti $L_{2,3}$ edges obtained by EELS for anatase, rutile, and the nanotube. All the spectra have a similar form. They are composed of two main contributions, namely, the L_3 and L_2 edges, separated by the $2p$ core-hole spin-orbit coupling of around 5 eV. The L_3 and L_2 edges are then both subdivided into two edges by the strong crystal-field splitting arising from the surrounding oxygen atoms. Figure 3 shows the calculated spectra using a crystal-field multiplet code for a Ti^{3+} ion and a Ti^{4+} ion in both an octahedral site and with tetrahedral symmetry.[13,15,16] For the Ti^{3+} ions, the spectrum corresponds to the electric dipolar allowed transition from the $3d^1$ ground state to a $\underline{c}3d^2$ final state where $\underline{c}$ denotes a Ti $2p$ core hole and $3d^n$ denotes n electrons in a Ti $3d$ orbital. Spectra for Ti^{4+} compounds correspond to transitions from a $3d^0$ ground state to a $\underline{c}3d^1$ final state. When comparing with these calculations and previously reported results for Ti^{3+} edges,[17–19] we can rule out the presence of Ti^{3+} ions in the nanotube. The Ti L edges for a trivalent ground state are shifted toward lower energies by

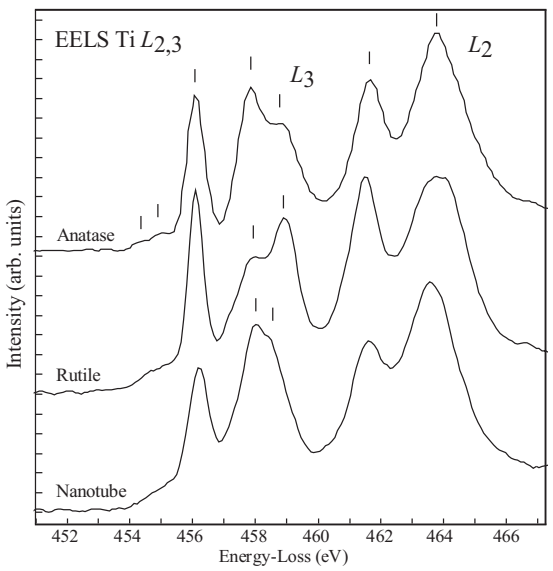

FIG. 2. Experimental EELS Ti $L_{2,3}$ main edges for anatase-, rutile-, and the titania-based nanotube. Energy range has been set at 456 eV at the sharper L_3 line for rutile.

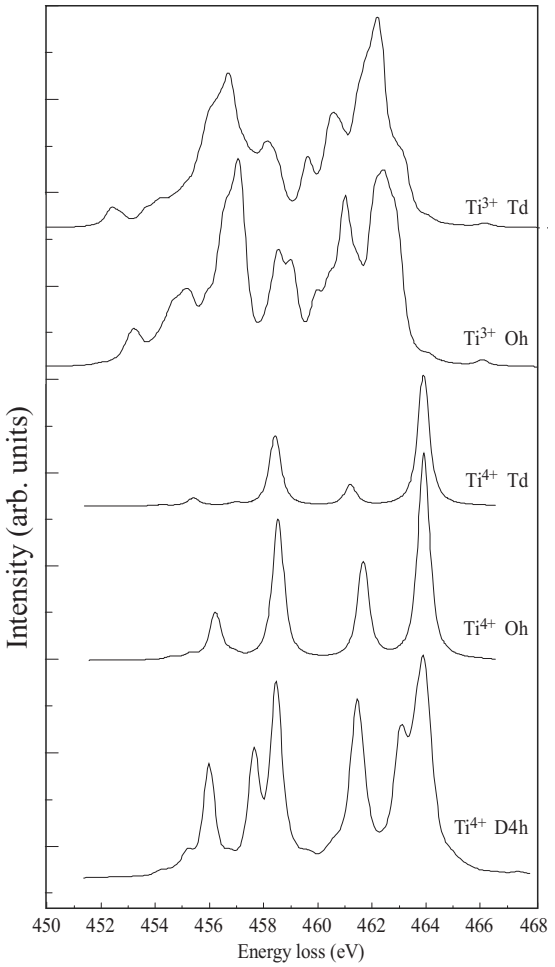

FIG. 3. Simulated EELS Ti $2p$ spectra for a Ti^{3+} ground state and a Ti^{4+} ground state in tetrahedral and octahedral symmetry. In this example, the crystal-field splitting has been set to $|10Dq| = E(e_g) - E(t_{2g}) = 1.8$ eV, typical value for transition-metal oxide. An Ti^{4+} ground state in lower symmetry showing "fortunate" agreement with the rutile experimental data is also shown. In the latter case, a crystal-field subsplitting of Ds=−90 meV and Dt =−140 meV have been set. Spectra have been aligned in accordance with the experimental energy.

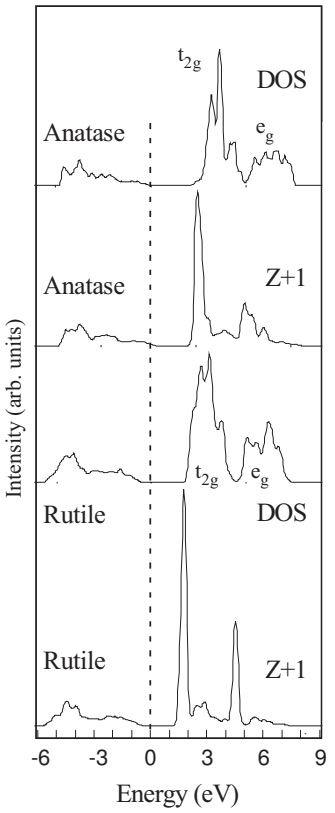

FIG. 4. DFT-LDA electronic structure for the anatase and rutile. Only the Ti $3d$ projected density of state are shown.

around 1.5 eV and show drastically different fine structure from that of tetravalent Ti. Equally the fine structure of tetrahedrally coordinated Ti^{4+} rules out this candidate structure. Experimental spectra of a $3d^0$ ion within Ti d symmetry, such as that of CaF_2, confirm this.[20] We can therefore conclude that the three phases, including the nanotubes, are composed of tetravalent titanium in an octahedral symmetry.

We find that the experimental splitting of the L_2 line for anatase and the tube are of comparable magnitude (around 2 eV), the splitting for rutile being somewhat larger (2.3–2.4 eV). Estimation of the separation between the t_{2g} and e_g orbitals is not straightforward with the splitting of the L lines. Nevertheless, comparisons with previously reported crystal-field[20] or charge-transfer multiplet (CTM) calculations[21] give an estimation of the required correction. According to Crocombette and Jollet,[21] the orbital separation in the ground state is reduced to around 1.8 eV for anatase (and thus presumably the same value for the nanotube) and to around 2 eV for rutile.

Additional splitting is observed in the main peak of the L_3 lines, usually attributed to be of primarily e_g character.[22] The rutile has a shoulder at the lower-energy side while anatase and the nanotube have a shoulder at the higher-energy side with different energy splittings. The fine structure for the rutile, including this additional splitting, can be simulated using a lower symmetry for the ground state (see Fig. 3 and Ref. 15). Nevertheless, according to Crocombette and Jollet,[21] the fine structure for rutile, anatase, and brookite cannot be properly simulated using a crystal-field or charge-transfer model, taking into account only the first- or second-neighboring shell. Indeed, we have not been able to mimic the fine structure of the anatase or the nanotube by using the correct crystal-field parameters. Finkelstein *et al.*[22] observe that the e_g peak of the L_3 line of rutile matches well with the Ti $3d(e_g)$ unoccupied density of states (DOS) for the ground state of rutile (see Fig. 4). Unfortunately we believe that this band approach to the interpretation of the Ti $L(e_g)$ fine structure is not very transferable to many titanium oxides. For instance, the anatase L_3 line does not match with the calculated unoccupied DOS. Incorporation of an unscreened core hole through the so-called $Z+1$ approximation[23] shows strong excitonic character and does not lead to a better match with experimental data (see Fig. 4). The Ti 2p EELS subsplitting involves a strong interplay between $3d(e_g)$ band formation and correlation effects, and cannot be used to estimate the crystal-field distortion, at least, if limitations of a

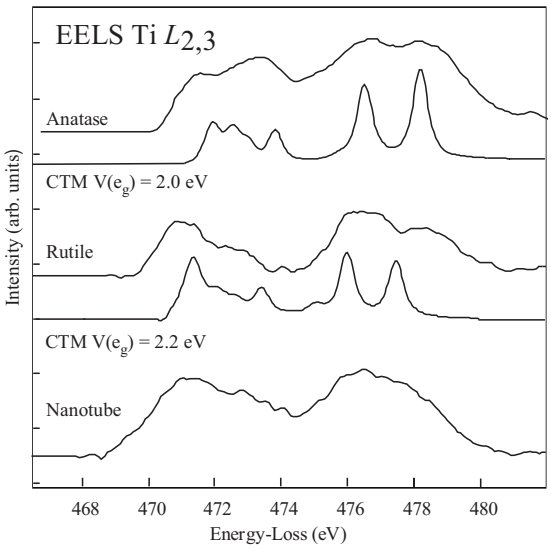

FIG. 5. Experimental EELS Ti $L_{2,3}$ satellite edges for anatase-, rutile-, and the titania-based nanotube. CTM calculations for two hybridization strengths $V(e_g)$ are also reproduced. The CTM edges have been rigidly 2.5 eV shifted to the higher energy.

single-particle approach are not overcome in the calculation.[24] Differences between anatase, rutile, and the nanotube show only that the octahedra have different long-range connectivity.[25]

B. Ti $L_{2,3}$ charge-transfer satellites

Figure 5 shows detail of the Ti $L_{2,3}$-edge spectra at a higher-energy range starting 10 eV above the onset of the edges. One can clearly see four main excitations. The spectra for rutile and the tube are very similar (the tube spectrum being slightly broader). However the anatase spectroscopic signature is different, the second and fourth peak being more intense and the whole signature shifted upward in energy by around 0.5 eV. To extract these signatures, we first removed the plural scattering contribution, using either a Fourier-ratio technique or a maximum-likelihood deconvolution technique (the low loss spectra being acquired in the same area). We then fitted the EELS spectra with a Hartree-Fock atomic calculation of the edges. The matching window is chosen to lie well after the onset of the edges, i.e., between 490 and 510 eV. The procedure seems stable as a function of the thickness and the extracted signature for rutile and anatase is in good agreement with that published by van der Laan[26] using XAS and another extraction technique. In the earlier paper[26] these excitations were ascribed to excitonic satellites. Later, Okada and Kotani[27] attributed these transitions to charge-transfer satellites.

We have performed simulations of these spectra using a simplified version of a single impurity Anderson model.[13] Within a simulation of a TiO_6 cluster, there are several adjustable parameters that can be varied to fit the experimental data. These include the charge-transfer energy $\Delta_i = E(d^{n+1}\underline{L}) - E(d^n)$, where $\underline{L}$ denotes a hole in the oxygen $2p$ orbitals and $E(d^{n+1}\underline{L})$ and $E(d^n)$ denote the multiplet averaged energies of the charge transfer and ionic configurations, respectively. The crystal-field splitting 10Dq and the corresponding mixing factors $V(e_g)$ and $V(t_{2g})$ between the Ti $3d$ and O $2p$ orbitals are also included. We have fixed $V(e_g) = -2V(t_{2g})$, as this has already been demonstrated to give good results.[13] Correlation effects are also present through the on-site $3d$-electron repulsion energy U_{dd} and the core-hole attraction U_{pd}. Details of the calculation techniques can be found in references.[13,28–31] The difference $U_{dd} - U_{pd}$ is important since it relates to the charge-transfer energy in the final state $\Delta_f = E(\underline{c}d^{n+1}\underline{L}) - E(\underline{c}d^n)$, where $\underline{c}$ denotes the Ti $2p$ core hole, through the estimation $\Delta_f = \Delta_i - (U_{pd} - U_{dd})$.[28] The intensity of the charge-transfer excitations with respect to the main peak are indeed related to the difference in energy between Δ_i and Δ_f (for $\Delta_i = \Delta_f$, no satellite peaks should be observed in the EELS spectrum[13]). We have therefore chosen $\Delta_i = 4$ eV and $\Delta_f = 1$ eV, corresponding to a large $U_{pd} - U_{dd} = 3$ eV, which was necessary in order to obtain an intense simulated charge-transfer peak. This difference is slightly larger that the 1–2 eV traditionally used for transition-metal oxides,[13] including work on titanium-oxide materials.[32] However Crocombette and Jollet[21] also used these parameters to simulate Ti $2p$ XAS data. Parlebas *et al.*[33] also proposed that the XPS charge-transfer satellites are intense due to the strong attraction of the Ti $2p$ core hole. Based on this experimental data, they estimated $U_{pd} \approx 8$ eV, in agreement with our value (see Table I).

Our calculations show that the choice of Δ_i only has a very weak influence on the position and shape of the satellite

TABLE I. Parameters used to simulate the Ti excitations in an Anderson impurity model. U_{cd} notes the core-hole attraction and can either be U_{pd} or U_{sd} depending on the excitations ($2p$ or $1s$). The R stands for the reduction parameter of the Slater integral ($R=1$ means no reduction). Other parameters have been defined in the text. Note that a slightly modified impurity model has been used by the authors (as discussed in the text).

Reference	Spectroscopic excitations	Material	U_{cd} (eV)	U_{dd}(eV)	$U_{cd} - U_{dd}$ (eV)	Δ_I (eV)	$V(e_g)$ (eV)	R	10Dq (eV)
34	XAS Ti $1s$	Rutile	$U_{sd}=6.0$	4.0	2.0	3.4	3.5	0.85	1
32	XPS Ti $2p$	Ti_2O_3	$U_{pd}=5.3$	4.5	0.8	6.5	3.0	0.7–0.9	0.5
33	XPS Ti $2p$	Rutile	$U_{pd}=7.0$	5.0	2.0	4.0	3.46		
27	XAS-XPS Ti $2p$	Rutile	$U_{pd}=6.0$	4.0	2.0	3.0	3.0	0.85	1.7
21	XAS Ti $2p$	Anatase, rutile	$U_{pd}=8.0$	6.0	2.0	4.0	3.6	0.6	
This study	EELS Ti $2p$	Anatase, rutile	$U_{pd}=8.0$	5.0	3.0	4.0	2.0–2.2	0.9	1.8

peaks. Increasing Δ_i from 2 to 4 eV shifts the satellite peak by only 0.5 eV. As mentioned by Nadai *et al.*,[31] the weak influence of the charge-transfer energy is particularly effective if a truncated basis is used (addition of more configurations, such as $d^2\underline{L}^2$ and $d^3\underline{L}^3$, may change this).

With this choice of energy set (U_{dd}=5 eV, U_{pd}=8 eV, and Δ_i=4 eV), the driving-force parameter controlling the energy position and shape of the satellite peaks are the hybridization strengths. In the case of a truncated basis limited to two configurations $3d^0$ and $3d\underline{L}^1$, Hamiltonian describing the final state of the EELS excitation can be approximated by $Hf=\begin{pmatrix} 0 & \mathrm{Veff} \\ \mathrm{Veff} & \Delta_f \end{pmatrix}$, where $\mathrm{Veff}=\sqrt{4\times V(e_g)^2+6\times V(t_{2g})^2}$, representing an average hybridization strength and $\Delta_f=\Delta_i-(U_{pd}-U_{dd})$ is the charge-transfer energy in the final state. After diagonalization of the matrix, the difference in energy between the main peak and the satellite peak is then estimated at $\Delta E=\sqrt{\Delta_f^2+4\times \mathrm{Veff}^2}$. In the case of the titanium dioxide, the charge-transfer energy in the final state is very weak compared to the hybridization strength. Indeed, with the chosen parameters Δ_f=1 eV and Veff=5 eV, the energy difference is then close to $\Delta E=2\times$Veff and the position in energy of the satellite peak scales strongly with the hybridization. One can see in Fig. 5 that a small variation in $V(e_g)$ from 2 to 2.2 eV shifts the spectra by around 0.5 eV and changes the relative intensity of the charge-transfer peak. In particular, the difference between rutile and the nanotube on one side and anatase on the other are qualitatively simulated. These hybridization values are smaller than those used conventionally. Crocobette and Jollet[21] used a $V(e_g)$ of 3.6 eV but also introduced a strong reduction in the Slater integral that we have not used. Lefevre *et al.*[34] suggest from Ti-K prepeak analysis a $V(e_g)$ of around 3.6 eV. If we use this value, our calculated satellite-peak energy position is around 4 eV too high. With our chosen parameters, the energy position of the satellite peak is only around 2 eV too low. We have searched for an alternative balance between greater hybridization strength and a reduction factor of the Slater integral but no better matches with experiment have been obtained. We conclude that the small difference in the charge-transfer satellite is due to tiny changes in the hybridization strength between these compounds.

Based on these two configuration $3d^0$ and $3d^1\underline{L}$ models, the difference in the *d*-band population between rutile and the titanate nanotubes on the one hand, and anatase on the other hand, is very small and estimated to be around $0.02e^-$. Based on the two configurations Anderson impurity model, the weight of the $d^1\underline{L}$ configuration is estimated at 28% for the rutile and the nanotube, and 30% for the anatase. Crocombette *et al.*[21] find comparable tiny difference of $0.03e^-$ in the Ti *d* orbitals using a slightly different technique of charge-transfer multiplet calculation. A survey of the literature of the density-functional theory (DFT)-calculated population is of little help since most of the studies confirm that the difference in hybridization between anatase and rutile is very small and not meaningful in the scheme of the DFT-local-density approximation (LDA). The Ti $3d$ occupation is around one electron for titanium dioxide, according to both charge-transfer multiplet calculations in a nontruncated basis and to DFT calculations.[35] The smaller absolute amount of d electrons found here is due to the use of a two configuration basis.

C. O-K edges

Figure 1 shows EELS O-K edges for the three phases. Both the anatase and rutile spectra match well with published XAS spectra[25] and exhibit a strong prepeak due to the Ti $3d$-O $2p$ hybridization. The prepeak splitting is measured at 2.5 eV for anatase and 2.75 eV for rutile, confirming a somewhat higher crystal-field splitting for the rutile structure. For the nanotube the splitting is around 2.5 eV, closer to that of anatase. This confirms that the crystal-field splitting of the titanate tubes is close to that of anatase. The O-K prepeak is broader for the nanotube. Since hybridization between the O $2p$ and Ti $3d$ orbitals are nearly the same for the three phases, this broadening may come from the presence of some hydroxyl bonding and be indicative of a less well-defined local structure.

IV. CONCLUSIONS

We have performed electron-energy-loss spectroscopic studies of the oxygen K and titanium $L_{2,3}$ edges of anatase-, rutile-, and titania-based nanotubes. The nanotubes are composed of $(TiO_6)^{8-}$ polyhedra, i.e., Ti^{4+} ions in octahedral symmetry. The e_g to t_{2g} separation is around 1.8 eV, comparing well with crystal fields of anatase. The subsplitting of the main e_g peak of the Ti L_3 edges for these oxides cannot be interpreted simply in terms of a crystal-field splitting or using a band approach. The fine structure of the L_3 lines of the nanotube does not match that of anatase or rutile, suggesting that the TiO_6 polyhedra in the tubes have different long-range connectivity to that of anatase and rutile. Charge-transfer satellites show that the weight of the ligand hole configuration in the ground state for the nanotubes is more comparable with that of rutile, indicating that the layered structure shows a lot of hybridization. Measurement of EELS charge-transfer peaks, shown here at a nanometer scale for the titanate nanotube, may be useful in many other contexts to evaluate locally the *d* or *f* band occupations. Potential examples include transition-metal ions at the vicinity of interfaces for spintronic multilayers or encaged rare-earth atoms in carbon-based nanostructures where local charge transfer is of particular interest.

[1] A. Fujishima and K. Honda, Nature (London) **238**, 37 (1972).
[2] T. Kasuga, M. Hiramatsu, A. Hoson, T. Sekino, and K. Niihara, Langmuir **14**, 3160 (1998).
[3] B. D. Yao, Y. F. Chan, X. Y. Zhang, W. F. Zhang, Z. Y. Yang, and N. Wang, Appl. Phys. Lett. **82**, 281 (2003).
[4] W. Wang, O. Varghese, M. Paulose, and C. A. Grimes, J. Mater. Res. **19**, 417 (2004).
[5] Q. Chen, G. H. Du, S. Zhang, and L.-M. Peng, Acta Crystallogr.

Sect. B: Struct. Sci. **58**, 587 (2002).
[6] S. Zhang, L. M. Peng, Q. Chen, G. H. Du, G. Dawson, and W. Z. Zhou, Phys. Rev. Lett. **91**, 256103 (2003).
[7] Z. Y. Yuan and B. L. Su, Colloids Surf., A **241**, 173 (2004).
[8] J. Yang, Z. Jin, X. Wang, W. Li, J. Zhang, S. Zhang, X. Guo, and Z. Zhang, Dalton Trans. **2003**, 3898.
[9] M. Zhang, Z. S. Jin, J. W. Zhang, X. Y. Guo, J. J. Yang, W. Li, X. D. Wang, and Z. J. Zhang, J. Mol. Catal. A: Chem. **217**, 203 (2004).
[10] R. Ma, Y. Bando, and T. Sasaki, Chem. Phys. Lett. **380**, 577 (2003); C.-W. Peng, M. Richard-Plouet, M.-C. Tsai, C.-Y. Lee, H.-T. Chiu, P.-E. Petit, H.-S. Sheu, S. Lefrant, and L. Brohan, Cryst. Growth Des. **8**, 3555 (2008).
[11] P. Umek, P. Cevc, A. Jesih, A. Gloter, C. P. Ewels, and D. Arcon, Chem. Mater. **17**, 5945 (2005).
[12] O. Stephan, A. Gloter, D. Imhoff, M. Kociak, C. Mory, K. Suenaga, M. Tence, and C. Colliex, Surf. Rev. Lett. **7**, 475 (2000).
[13] F. M. F. de Groot, J. Electron Spectrosc. Relat. Phenom. **67**, 529 (1994).
[14] A. Gloter, A. Douiri, M. Tence, and C. Colliex, Ultramicroscopy **96**, 385 (2003).
[15] F. M. F. de Groot, J. C. Fuggle, B. T. Thole, and G. A. Sawatzky, Phys. Rev. B **42**, 5459 (1990).
[16] R. D. Cowan, *The Theory of Atomic Structure and Spectra* (University of California Press, Berkeley, 1981); P. H. Butler, *Point Group Symmetry Applications: Methods and Tables* (Plenum, New York, 1981); The programs have then been modified by B. T. Thole, H. Ogasawara, and F. M. F. de Groot and have kindly been provided by F. M. F. de Groot via http://www.anorg.chem.uu.nl/
[17] F. M. F. de Groot, M. O. Figueiredo, M. J. Basto, M. Abbate, H. Petersen, and J. C. Fuggle, Phys. Chem. Miner. **19**, 140 (1992).
[18] M. Abbate, F. M. F. de Groot, J. C. Fuggle, A. Fujimori, Y. Tokura, Y. Fujishima, O. Strebel, M. Domke, G. Kaindl, J. van Elp, B. T. Thole, G. A. Sawatzky, M. Sacchi, and N. Tsuda, Phys. Rev. B **44**, 5419 (1991).
[19] D. A. Muller, N. Nakagawa, A. Ohtomo, J. L. Grazul, and H. Y. Hwang, Nature (London) **430**, 657 (2004).
[20] F. M. F. de Groot, J. C. Fuggle, B. T. Thole, and G. A. Sawatzky, Phys. Rev. B **41**, 928 (1990).
[21] J. P. Crocombette, and F. Jollet, J. Phys.: Condens. Matter **6**, 10811 (1994).
[22] L. D. Finkelstein, E. I. Zabolotzky, M. A. Korotin, S. N. Shamin, S. M. Butorin, E. Z. Kurmaev, and J. Nordgren, X-Ray Spectrom. **31**, 414 (2002).
[23] M. D. Segall, P. L. D. Lindan, M. J. Probert, C. J. Pickard, P. J. Hasnip, S. J. Clarck, and M. C. Payne, J. Phys.: Cond. Matter **14**, 2717 (2002).
[24] G. Fronzoni, R. De Francesco, M. Stener, and M. Causa, J. Phys. Chem. B **110**, 9899 (2006).
[25] R. Ruus, A. Kikas, A. Saar, A. Ausmees, E. Nommiste, J. Aarik, A. Aidla, T. Uustare, and I. Martinson, Solid State Commun. **104**, 199 (1997).
[26] G. van der Laan, Phys. Rev. B **41**, 12366 (1990).
[27] K. Okada and Akio Kotani, J. Electron Spectrosc. Relat. Phenom. **62**, 131 (1993).
[28] Z. Hu, G. Kaindl, S. A. Warda, D. Reinen, F. M. F. de Groot, and B. G. Müller, Chem. Phys. **232**, 63 (1998).
[29] Z. Hu, Chandan Mazumdar, G. Kaindl, F. M. F. de Groot, S. A. Warda, and D. Reinen, Chem. Phys. Lett. **297**, 321 (1998).
[30] Z. Hu, M. S. Golden, J. Fink, G. Kaindl, S. A. Warda, D. Reinen, P. Mahadevan, and D. D. Sarma, Phys. Rev. B **61**, 3739 (2000).
[31] C. De Nadai, A. Demourgues, J. Grannec, and F. M. F. de Groot, Phys. Rev. B **63**, 125123 (2001).
[32] T. Uozumi, K. Okada, A. Kotani, R. Zimmermann, P. Steiner, S. Hüfner, Y. Tezuka, and S. Shin, J. Electron Spectrosc. Relat. Phenom. **83**, 9 (1997).
[33] J. C. Parlebas, J. Phys. I **2**, 1369 (1992).
[34] P. Le Fèvre, H. Magnan, D. Chandesris, J. Jupille, S. Bourgeois, W. Drube, H. Ogasawara, T. Uozumi, and A. Kotani, J. Electron Spectrosc. Relat. Phenom. **136**, 37 (2004).
[35] Y. Joly, D. Cabaret, H. Renevier, and C. R. Natoli, Phys. Rev. Lett. **82**, 2398 (1999).